

# A Quality-Centric Framework for Generic Deepfake Detection

Wentang Song, Zhiyuan Yan, Yuzhen Lin, Taiping Yao, Changsheng Chen, *Senior Member, IEEE*, Shen Chen, Yandan Zhao, Shouhong Ding, Bin Li, *Senior Member, IEEE*

**Abstract**—This paper addresses the generalization issue in deepfake detection by harnessing forgery quality in training data. Generally, the forgery quality of different deepfakes varies: some have easily recognizable forgery clues, while others are highly realistic. Existing works often train detectors on a mix of deepfakes with varying forgery qualities, potentially leading detectors to short-cut the easy-to-spot artifacts from low-quality forgery samples, thereby hurting generalization performance. To tackle this issue, we propose a novel quality-centric framework for generic deepfake detection, which is composed of a Quality Evaluator, a low-quality data enhancement module, and a learning pacing strategy that explicitly incorporates forgery quality into the training process. The framework is inspired by curriculum learning, which is designed to gradually enable the detector to learn more challenging deepfake samples, starting with easier samples and progressing to more realistic ones. We employ both static and dynamic assessments to assess the forgery quality, combining their scores to produce a final rating for each training sample. The rating score guides the selection of deepfake samples for training, with higher-rated samples having a higher probability of being chosen. Furthermore, we propose a novel frequency data augmentation method specifically designed for low-quality forgery samples, which helps to reduce obvious forgery traces and improve their overall realism. Extensive experiments show that our method can be applied in a plug-and-play manner and significantly enhance the generalization performance.

**Index Terms**—Deepfake Detection, Multimedia Forensics, Forgery Quality Evaluation

## I. INTRODUCTION

DEEFAKE techniques have experienced rapid advancements in recent years, providing a new way of entertainment. Unfortunately, this technology is also broadly misused to spread false misinformation and even bring political influence. To prevent the abuse of deepfake, it is increasingly crucial to develop a reliable deepfake detector. Most earlier deepfake detectors [1]–[6] achieve satisfied and promising detection results in the within-domain evaluation scenario, where the distributions of the training and testing data are

Wentang Song, Yuzhen Lin, Changsheng Chen, and Bin Li are with Guangdong Provincial Key Laboratory of Intelligent Information Processing, Shenzhen Key Laboratory of Media Security, and the SZU-AFS Joint Innovation Center for AI Technology, Shenzhen University, Shenzhen 518060, China (e-mail: 2018132120@szu.edu.cn; linyuzhen2020@email.szu.edu.cn; cschen@szu.edu.cn; libin@szu.edu.cn)

Zhiyuan Yan is with the School of Electronic and Computer Engineering, Peking University, Shenzhen Graduate School, Shenzhen 518055, China (e-mail: zhiyuanyan@stu.pku.edu.cn).

Taiping Yao, Shen Chen, Yandan Zhao, and Shouhong Ding are with YouTu Lab, Tencent, Shanghai 200233, China (e-mail: taipingyao@tencent.com; kobeschen@tencent.com; yandanzhao@tencent.com; ericshding@tencent.com).

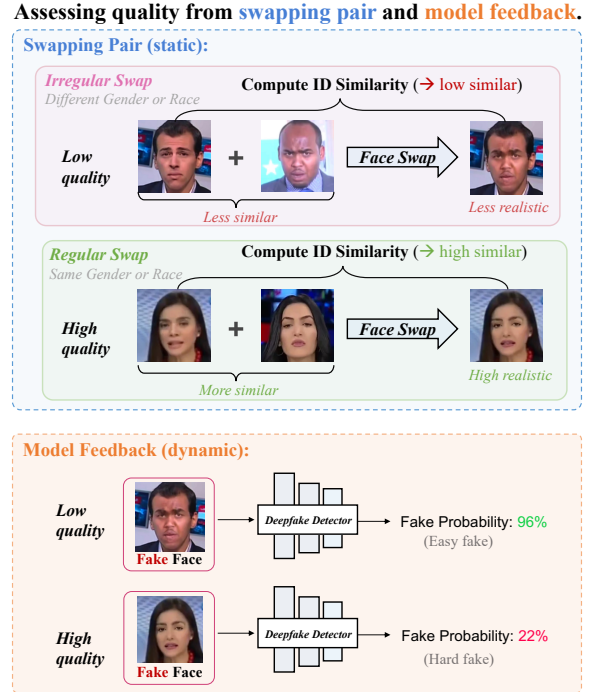


Fig. 1. Illustration of the proposed forgery quality assessment. We assess the forgery quality from two views: swapping pairs (static) and model feedback (dynamic). Our quality-centric framework enables the detector to progressively learn the deepfake artifacts from easy (lower quality) to hard (higher quality), avoiding the potential shortcuts on easy artifacts from low-quality samples, thereby improving the generalization.

similar. However, when encountering cross-domain evaluation, with previously unseen forgery methods or data sources, the performance of these models will drop significantly [7]. Thus, the generalization ability of these prior works is still limited.

One reason for the generalization issue is the model's shortcuts [8] on the easy-to-spot artifacts from the training samples with low forgery quality [9]–[11]. For instance, the “irregular swap” fake samples are frequently observed in FF++ (a common training set) but rarely in CDF-v2 (a common testing set). “Irregular swaps” is firstly noticed by [11], where face-swapping involves pairs with distinct facial attributes, such as differences in race or gender. These irregular swaps often severely distort the human facial structure, leading to lower-quality fake samples. As illustrated in Figure 1, we see that when “irregular swaps” occur (*i.e.*, swapping a white face with a black face or a female face with a male face), the easy-to-recognized deepfake samples are generated. To

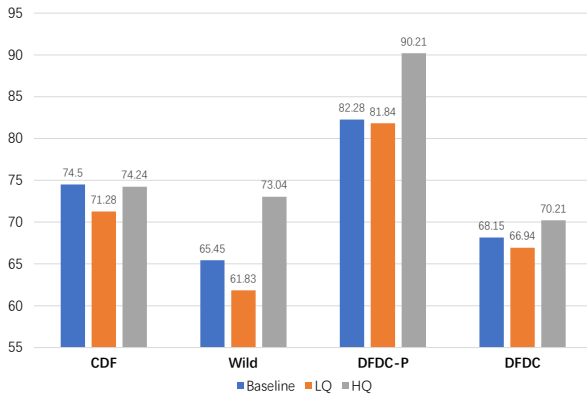


Fig. 2. Comparison of generalization performance of models trained using data of different quality. Baseline refers to using all data to train the model, LQ only means that it only uses low static quality data for training, and HQ stands for training using high static quality data.

verify the impact of these lower forgery quality fakes on the model’s generalization, we selectively choose samples with different forgery qualities for training the same detector (*i.e.*, Xception [12]). Results in Figure 2 verify that these low static quality samples indeed hurt the model’s generalization, especially in the Wild [13] and DFDC-P [14] datasets, where simply training with higher-quality samples can obtain about 10% improvement in the generalization performance. However, most existing methods often train detectors on a mix of qualities of deepfake data, which might inevitably struggle with this issue (similar to the “baseline” in Figure 2), as they treat all data as the same and ignore the impact of different forgery qualities.

These observations motivate us to treat training data with forgery qualities differently. To this end, we need to address three critical considerations first: **Question 1**: *How can we assess the quality level of a sample?* **Question 2**: *How to deal with low-quality fake data?* **Question 3**: *How can we maximize the utilization of all types of data?* In the following content, we will answer the above research questions in detail.

For **Question 1**, our solution is to assess the forgery quality from the perspective of data (in a statical view) and that of a detection model (in a dynamical view), as illustrated in Figure 1. **From the static view**, we concentrate on *swapping pairs* in the face-swapping process, with the assumption that obtaining paired data is feasible. For a given deepfake generator, similar IDs for swapping can potentially yield more realistic deepfakes (see Fig. 1 for illustration). The rationale behind this is that: for a high static quality deepfake sample, the visual forgery artifacts should be as small as possible, meaning that the facial structure of the face should be natural and seamless. On the contrary, the low static quality sample contains obvious visual artifacts, leading to significant damage to the facial structure. Therefore, we can assess the forgery quality statically by focusing on the swapping pairs. To achieve this, we employ the face recognition network (*i.e.*, ArcFace [15]), taking both the fake and the corresponding real samples as input (with identical backgrounds), and then compute the cosine similarity of the obtained features. If the similarity is low, we can

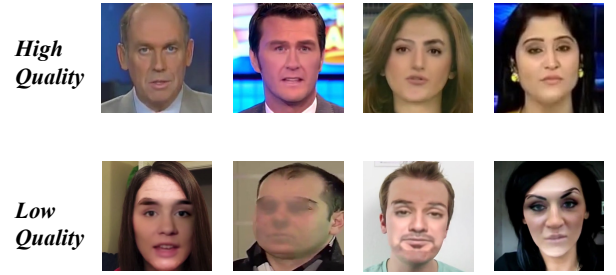


Fig. 3. Illustration of **fake examples** with different static quality within the FF++ dataset (training set). Intuitively, training with low static quality samples can lead the model to learn the shortcut and thus hurt the model’s generalization.

argue that the fake should be of low static quality. **From the dynamic view**, we assess the forgery quality from the model’s feedback on each sample during training; a lower prediction probability indicates a higher dynamic score, as the fakes are more challenging to detect (see Figure 1 for illustration). Finally, we combine both the static and dynamic assessment results to produce the Forgery Quality Score (FQS) for sample selection. *Note that, unless otherwise specified, low-quality and high-quality data refer to samples characterized by low FQS and high FQS, respectively.*

For **Question 2**, our solution is to reduce the obvious forgery traces of the low-quality samples and enhance their realism, rather than directly discarding them. To achieve this, we propose Frequency Data Augmentation (FreDA), which retains the low-frequency features from real faces and reconstructs new augmented samples by integrating the high-frequency features from the original fake samples. Consequently, the facial structure of augmented low-quality samples is improved, transforming them into relatively high-quality samples. FreDA operates based on the fact that low-frequency components in an image represent the overall facial structure, which are crucial for maintaining the face’s semantic integrity. Since low-frequency regions dominate a fake face and can vary significantly between samples, detectors trained on these features often learn non-generalizable artifacts. In contrast, high-frequency components capture finer details. They are more consistent and robust forgery indicators. FreDA aims to combine these high-frequency parts (more general) of the fake and the low-frequency parts (semantic facial structure) of the real, thereby resulting in a new (more realistic) fake.

For **Question 3**, our solution is to employ the curriculum learning technology to guide the model to start with easy samples and then gradually focus more on challenging samples. Specifically, we compute the FQS values for each sample and use this value to sample training data during the training process. The higher the FQS score, the more likely it is to be sampled into the hard sample pool. As training progresses, we gradually reduce the number of training samples to focus the model’s attention on harder samples, guiding the progression of the training subsets from easy to hard. Concurrently, we apply FreDA operations to low-quality samples to increase their hardness and enhance the diversity of the training data. In this manner, we can fully leverage training data with all

qualities. Experimental results demonstrate that our method can improve both the within- and cross-dataset performance of various kinds of deepfake detectors in a plug-and-play manner.

Compared with our preliminary work [16], this paper mainly makes two additional major contributions. **Firstly**, the focus is different. [16] mainly concentrates on *image quality*, whereas our work is more centered on *forgery quality*. Specifically, the key technical difference lies in the design of the static prior knowledge part. [16] employs the Image Forgery Quality Assessment network (IFQA) to consider the impact of post-processing on image quality but fails to take into account irregular face-swapping scenarios (forgery quality). In this paper, we incorporate the feature similarity measured by ArcFace to evaluate the quality of swapped faces. By making use of the ArcFace score, we can refine the selection of hard samples more accurately, considering samples with better-swapped faces as more challenging ones. **Secondly**, we have also enhanced how we handle easy samples. While DFFC adopts common data post-processing methods such as JPEG compression and Gaussian blurring for easy samples, we devise a novel data augmentation approach called FreDA, explicitly leveraging frequency domain processing, effectively enhancing all types of forged samples (FF++, BI-based, and SBI-based); therefore it further boosts the generalization capability. Notably, our method outperforms the baseline [12], [17], [18] by about 10% on average across several widely-used evaluation datasets, such as Celeb-DF [19] and DFDC [20].

Our main contributions are as follows:

- We design a novel quality-centric training framework based on curriculum learning, which is composed of a Quality Evaluator, a low-quality data enhancement module, and a learning pacing strategy, encouraging the model to learn the deepfake artifacts gradually from easy to hard according to quality assessment.
- We propose an assessment method combining both static and dynamic views to obtain the Forgery Quality Score (FQS), which allows us to rank the hardness of the training samples, thereby implementing the training sample selection.
- For low-quality samples, we propose Frequency Data Augmentation (FreDA) to reduce the obvious forgery traces and thereby enhance the realism of the augmented low-quality data, rather than directly discarding them. FreDA can reduce the traces of forgery in forged samples. Using samples processed by FreDA enhances the model's generalization.
- Extensive experiments verify that the proposed framework significantly improves the generalization of the baseline model and can be applied in a plug-and-play manner.

## II. RELATED WORKS

### A. Deepfake Detection

Detecting deepfake videos has become an area of intense research due to the growing concern over the potential misuse of manipulated media content. Most works at an early stage, mainly focus on hand-crafted features, *e.g.*, eye-blinking [21],

inconsistencies [22] of head poses [23], and other visual biological artifacts. With the rapid development of deep learning, data-driven-based detectors [2] have shown better performance than the conventional hand-crafted approaches. Zhao *et al.* [24] used attention mechanisms to enhance the manipulated trace in deepfake videos. Yet, these approaches often suffer from poor generalization when there is a distribution shift between training and testing forgeries [25]–[27].

Existing works have sought to improve generalization from different directions. Below, we give a brief introduction by focusing on three key aspects:

**1) Forgery Artifact Learning:** A key challenge in deepfake detection is learning universal forgery traces that can be generalized across various manipulation methods. Several solutions, such as disentanglement learning [28], [29], reconstruction learning [30], [31] and inconsistent learning [32]–[37], have been proposed to learn general forgery artifacts. These methods aim to isolate the common characteristics of manipulated content, irrespective of the specific forgery technique employed. To illustrate, UCF [28] proposed a disentanglement-based framework to eliminate the overfitting of both forgery-irrelevant content and forgery-specific artifacts. UIA-ViT [32] used the self-attention mechanism to make the attention map between patch embeddings naturally represent the consistency relationship. FoCus [34] located forgery cues in unpaired faces and generated more accurate forgery images through a classification-attention region proposal module and a complementary learning module. CADD [37] used the identity inconsistency between the inner and outer faces for detection. Additionally, RECCE [30] proposed a reconstruction-based framework that performs self-reconstruction using only genuine samples for the learning of common forgery artifacts.

However, these approaches mostly operate at the spatial level but overlook frequency-level artifacts, which have been demonstrated to be crucial for detection [38]. To this end, several studies have incorporated frequency information to enhance the performance of detectors [38]–[42]. For example, Ricard *et al.* [39] show that convolution-based upsampling methods, commonly used in deepfake technologies, can result in a discrepancy in the spectral distribution between fake and real images and videos. To tackle this issue, the authors introduce a frequency-based approach that outperforms many widely used spatial-based methods. Moreover, learning-based frequency domain methods have also been extensively investigated. For instance, Qianet *et al.* [38] develop a set of learnable filters to adaptively mine frequency forgery clues using frequency-aware image decomposition. Additionally, Liuet *et al.* [40] utilize frequency domain information as the fourth channel, combining it with RGB domain information as input to the network. SFDG [41] proposed a space-frequency dynamic graph method to mine relational perception features in the spatial and frequency domains through dynamic graph learning. CD-Net [42] proposed a cross-domain face forgery detection framework that exploits the consistency of multi-frame correlation representation and complementary cues in RGB and frequency domains.

Additionally, several recent works [43]–[45] have proposed to leverage both local and global interactions to more ac-

curately capture forgery traces. DL [43] proposed to use segmentation maps to provide high-level semantic information clues of the image, combine them with noise maps to capture low-level clues, and finally combine the features of the two to distinguish fake faces. MSVT [44] combined the local and global features to mine more detailed spatial-temporal information and integrate multi-level features through the global-local Transformer. Furthermore, [46]–[48] leveraged contrastive learning to improve the detection performance of deepfake detectors.

**2) Data-level Augmentation:** Forgery augmentation techniques have proven to be highly effective in enhancing the generalization ability of deepfake detectors by encouraging the model to learn generic forgery artifacts. Pioneering works such as BI (Face X-Ray) [7] synthesized blended faces by replicating blending artifacts between pairs of pristine images with similar facial landmarks. I2G [49] employed a similar strategy, leveraging pair-wise self-consistency learning to identify inconsistencies within generated fake images. Later efforts, like SBI [10], focused on self-blending, selecting the same source and target faces to train models, while SLADD [50] utilized adversarial training to generate more challenging blending scenarios. AUNet [51] built relationships between action units and used tampered action unit prediction modules to generate feature-level pseudo samples. These approaches highlight the importance of augmenting data to expose models to diverse forgery examples. More recently, [52] and [53] have explored video-level blending for data augmentation. While these approaches have improved generalization, many methods, particularly those that focus on low-level blending artifacts, remain vulnerable to post-processing operations such as compression. For example, Yan *et al.* [9] demonstrated that compression could significantly degrade the performance of RGB-based augmentation methods like SBI [10] and Face X-Ray [7], highlighting the need for more robust detection frameworks.

**3) Quality-aware deepfake detection:** Another notable direction is to train the detector with different image qualities (combining both low quality compression images and high quality non-compression ones), aiming to learn the quality-irrelevant forgery artifacts [54]. Recent works [16], [55] proposed to investigate the correlation between the detection performance and the image quality. Additionally, [56] proposed a supper-resolution model for improving low quality deepfake detection. However, most existing works define the “quality” as the **image quality**, *e.g.*, whether the image is blurry or not. Although our framework is also quality-based, our focus is more on the **forgery quality**, *i.e.*, whether the deepfake image is realistic or not, rather than the image quality. In our framework, we propose to assess the forgery quality from two distinct aspects: swapping pairs and model feedback. We then design a curriculum-learning-based method to leverage samples with varying forgery qualities dynamically for training, guiding the detector to learn the deepfake samples from easy to hard gradually.

### B. Curriculum Learning

Curriculum Learning (CL) is a training paradigm that seeks to improve the performance of deep neural networks by presenting training data in a meaningful order or curriculum. In CL, training data is divided into several stages, each stage representing a different level of hardness. This approach allows the model to first learn easier examples and then gradually increasing the hardness of the examples. Early works on curriculum learning such as BabyStep [57], [58] have shown that providing the training proceeding with an optimized order of training sets can improve models’ performance. Subsequently, CL has been extended to incorporate different strategies such as dynamic curriculum learning [59] and self-paced learning [60]. Dynamic curriculum learning adjusts the hardness of examples dynamically during training based on the model’s performance, while self-paced learning encourages the model to learn from easier examples first and then gradually move to more complex examples. Self-Paced Learning (SPL) selects samples with smaller loss, and gradually increases the subset size over time to cover all the training data. Kong *et al.* [61] used a pre-trained model and the current model to calculate the loss of training samples as a definition of hardness. Furthermore, several studies have investigated the effectiveness of CL in various domains, including computer vision and natural language processing. Our method introduces a FQS inspired by the concept of SPL, selecting samples with higher FQS, and gradually decreasing the subset size over time to make the model focus on hard samples.

## III. METHOD

In this section, we introduce the proposed quality-centric framework. Our framework is inspired by curriculum learning that explicitly encourages the detection model to learn forgery artifacts gradually from easy to hard based on FQS. It emphasizes three key components: firstly, the evaluation of data quality; secondly, the data augmentation on low-quality data; and thirdly, the progressing use of quality-based data during training. To achieve this, we carefully design three specified modules to implement the framework: **1)** FQS is proposed as a metric to assess sample hardness during model training. It consists of two main components: *static scores* and *dynamic scores*. Static score (related to data) provides initial guidance at the start of model training. The weight of the static score gradually decreases as the training progresses. Dynamic score (related to model) is continuously updated based on the model’s feedback, to better screen samples throughout the training process; **2)** A FreDA module is proposed to enhance the forgery quality (“realism”) of the augmented low-quality fake samples; **3)** A pacing function is presented to control the pace of presenting data from easy to hard according to FQS. Each module will be detailed subsequently.

### A. Forgery Quality Score (FQS)

The hardness score plays a key role in curriculum learning as it describes the relative “hardness” of each sample in deepfake detection. In this work, we propose the FQS, which

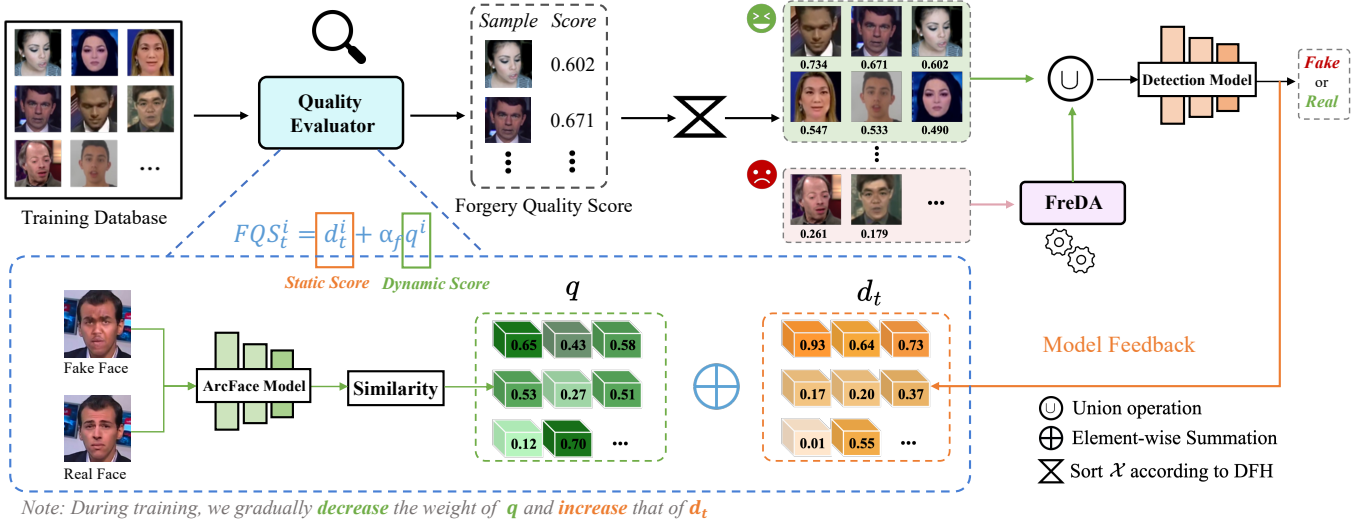


Fig. 4. Overall pipeline of the proposed method. To improve the existing data, we classify the samples through the Quality Evaluator module. For low-quality data, we use the FreDA module as shown Figure 5, to improve the quality of those samples.

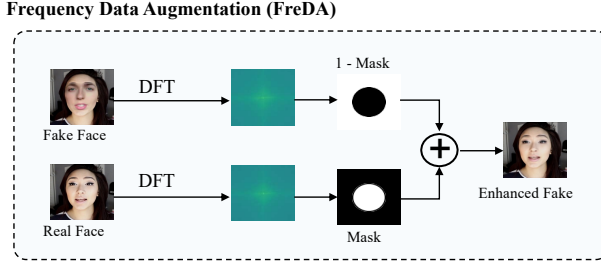


Fig. 5. For low-quality data, we employ the FreDA module to augment their forgery quality by reducing the easy-to-recognized artifacts and enhancing their realism.

considers the dynamic model behavior and the static facial data quality.

**Static quality.** The face recognition network learns rich facial feature representations through a large amount of external data. The features extracted through the face recognition network can capture detailed information and specific face attributes in the face image. High static quality deepfake images may have more accurate facial alignment, more realistic texture details, and more natural expression changes. Their features are more similar to the original images, causing the features extracted by the face network to be more similar to the original image features. On the contrary, low static quality deepfake images may have distortion, blur, or obvious forged details, resulting in features extracted by the face network being less similar to the original image features. For commonly used training datasets, there is a correspondence between deepfake videos and real videos. Taking advantage of such a fact, we input the fake image and its corresponding real image into a pre-trained face recognition network (Arcface), and calculate the cosine similarity of the features obtained by the model. The higher the similarity, the better the quality of the sample, and vice versa.

For an input fake image  $x_f^i$ , we obtain its corresponding

real image  $x_r^i$ , input it into the face recognition network  $G(\cdot)$ , and obtain two features  $g_f^i, g_r^i$ :

$$\begin{cases} g_f^i = G(x_f^i), \\ g_r^i = G(x_r^i). \end{cases} \quad (1)$$

After that, we calculate the cosine similarity between the two features as the ID similarity score  $q^i$  of  $x_f^i$ :

$$q^i = \text{Cosine}(g_f^i, g_r^i). \quad (2)$$

The similarity score  $q^i$  is used as the static quality for the forgery quality evaluation, as the more similar face-swapping pairs, the more realistic deepfake is created.

**Dynamic quality.** Let  $\mathcal{X} = (x^i, y^i)_{i=1}^N$  be the training dataset with  $N$  samples,  $x^i$  and  $y^i$  represent the  $i$ -th data and its ground-truth label, respectively. Let  $f(\cdot, \theta_t)$  be the deepfake detector model with the parameter  $\theta_t$  at  $t$ -th epoch. We regard the loss (*i.e.*, the binary cross-entropy loss denoted as  $l(f(x^i, \theta_{t-1}), y^i)$ ) of  $i$ -th sample at  $t-1$ -th epoch as an indicator for the current hardness of this sample judged by the current state of the model before conducting the training step. Thus, we propose the instantaneous hardness  $s_t^i$  that normalized the current loss with the learning rate  $\eta_t$ , formulated as:

$$s_t^i = l(f(x^i; \theta_{t-1}), y^i) \cdot \eta_{max} / \eta_t, \quad (3)$$

where  $\eta_{max}$  is the max learning rate during the training. We measure the dynamic hardness  $d_t^i$  through a moving average of the instantaneous hardness  $s_t^i$  over training history, defined and computed recursively as:

$$d_t^i = \begin{cases} \gamma \times s_t^i + (1 - \gamma) \times d_{t-1}^i, & \text{if } i \in H_t \\ d_{t-1}^i, & \text{otherwise,} \end{cases} \quad (4)$$

where  $\gamma \in [0, 1]$  is a discount factor, and  $H_t$  is the subsets of hard samples at  $t$ -th epoch selected by the pacing function.

Finally, we perform a weighted summation of the static quality and dynamic quality to obtain the FQS, formulated as:

$$FQS_t^i = d_t^i + \alpha_f q^i, \quad (5)$$

where  $\alpha_f$  is a balance weight. As the training progresses,  $\alpha_f$  will gradually decrease.

### B. Frequency Data Augmentation (FreDA)

Samples with low (static) quality typically exhibit more pronounced distortions and artifacts compared to high-quality samples. These distortions may include severe blurring or pixelation, leading to a loss of facial detail and clarity. Additionally, low-quality samples may suffer from color inconsistencies, where certain areas of the face appear unnaturally saturated or desaturated. These inconsistencies can be attributed to improper lighting conditions or inaccuracies in the image manipulation process. Furthermore, low-quality samples often display visually evident traces of tampering, such as mismatched facial features, unnatural facial expressions, or visible blending boundaries between different facial regions, as shown in Figure 3. Overall, these factors contribute to a diminished resemblance to the original face and make low-quality samples more discernible from genuine images. According to previous work [11], we find that for fake videos of FF++, 59.44% of them are created using swapping pairs with different races or genders. Using these samples to train the model will easily make the model overfit to these obvious forgery traces, which will be harmful to the generalization of the model. However, discarding samples with low (static) quality outright would lead to a reduction in the number and diversity of training data, potentially limiting the model's ability to generalize effectively. Therefore, it makes sense to explore an effective strategy to utilize low-quality samples for improving generalization performances.

For a face image, its low-frequency information typically corresponds to the overall structure, outline, and general range of the face, while the high-frequency information represents the texture and subtle features of the face. In the case of fake samples, discrepancies with real samples are predominantly concentrated in high-frequency areas, indicating that tampering traces are often found in high-frequency components.

For these low-quality samples, the facial structure is severely damaged. We can use the low-frequency part of the corresponding real sample of the fake sample as the low-frequency component of the blended image, and use the high-frequency part of the fake sample as the high-frequency component of the blended image. In this way, the obtained sample will preserve the facial structure without destruction, while also retaining traces of tampering-related forgery.

Specifically, given a sample  $x \in \mathbb{R}^{H \times W \times C}$  we perform a 2D fast Fourier transform (FFT) for each channel independently to get the corresponding frequency representation  $F$  as below:

$$F(u, v) = \sum_{h=0}^{H-1} \sum_{w=0}^{W-1} x(h, w) e^{-j2\pi(u \frac{h}{H} + v \frac{w}{W})}. \quad (6)$$

Further, we denote with  $M$  a mask, whose value is zero except for the center region:

$$M(u, v) = \begin{cases} 1, (u, v) \in [c_h - r : c_h + r, c_w - r : c_w + r] \\ 0, others \end{cases}, \quad (7)$$

where  $(c_h, c_w)$  is the center of the image and  $r$  indicates the frequency threshold that distinguishes between high- and low-frequencies of the original image. Given a low-quality sample  $x_f$ , we first find its corresponding real sample  $x_r$ , and then perform FFT on these two images to obtain  $F_f$  and  $F_r$ . We splice the high-frequency information of the fake sample  $x_f$  and the low-frequency information of the real sample  $x_r$  to obtain  $F_a$ . The formula is expressed as follows:

$$F_a = F_r \otimes M + F_f \otimes (1 - M), \quad (8)$$

where  $\otimes$  denotes element-wise multiplication. Perform iFFT changes on the obtained  $F_a$  and convert it to the RGB domain, and then obtain the FreDA image  $x_a$ . The frequency representation  $F$  can be transferred to the original RGB space via an inverse FFT (iFFT), which can be formulated as:

$$x(h, w) = \frac{1}{H \cdot W} \sum_{h=0}^{H-1} \sum_{w=0}^{W-1} F(u, v) e^{j2\pi(u \frac{h}{H} + v \frac{w}{W})}. \quad (9)$$

Compared with  $x_f$ ,  $x_a$  has a relatively complete facial structure while retaining the traces of forgery.

The proposed FreDA focuses on frequency-level augmentation and distinguishes itself from previous studies in the following ways. **Compared to frequency-based detectors:** FreDA aims to reduce the obvious forgery artifacts of a less realistic deepfake image and transform it into a realistic one at the frequency level, while previous frequency detectors [38], [40] mainly mine the frequency signals (e.g., high-frequency components) as the auxiliary information of the original RGB and encourage the detector to learn spatial-frequency anomalies. **Compared to augmentation-based detectors:** FreDA is targeted on deepfake data and designed to reduce the obvious fake artifacts of the deepfake data at the frequency level, while previous augmentation-based detectors [7], [10], [49], [50] mostly target the real data and simulate the fake blending artifacts to transform the real data into the (more realistic) pseudo-fake data.

Overall, our proposed FreDA is a novel frequency-level augmentation method that is distinct from both existing frequency detectors and augmentation-based detectors.

### C. Learning Pacing

To control the learning pace of presenting data from easy to hard, we design a pacing function to determine the sample pool  $\mathcal{X}'_t$  of training data according to FQS. Like human education, if a teacher presents materials from easy to hard in a very short period, students will become confused and will not learn effectively. Thus, we define a pacing sequence  $\mathbf{T} = [T_0, \dots, T_N]$  to represent  $n + 1$  milestones (i.e.,  $n$  episodes) in total training epoch  $T$ . During the first  $T_0$  epochs, we utilize all the samples in  $\mathcal{X}$  for the warm-up training. After epoch  $T_0$ , we only change the size of  $\mathcal{X}'_t$  at every milestone

$T_n$ . Specifically, at each epoch  $t$  of episode  $n$ , we select  $k_n$  samples with top FQS values in  $\mathcal{X}$  (i.e., hardest samples) as a hard sample pool  $H_t$ . Along with the training, we reduce the size of  $H_t$  by  $k_n \leftarrow \alpha_\beta \times k_{n-1}$  with discount factor  $\alpha_\beta$  to make it gradually focus on harder samples. To further enlarge the diversity of the data, we also select the  $E$  samples with bottom FQS values in  $\mathcal{X}$  (i.e., easiest samples) as an easy sample pool  $E_t$  and then conduct *FreDA* on them. Finally, we get the sample pool  $\mathcal{X}'_t$  by mixing the  $H_t$  and *FreDA*( $E_t$ ), i.e.,  $\mathcal{X}'_t \leftarrow H_t \cup \text{FreDA}(E_t)$ . After that, we sample mini-batch in  $\mathcal{X}'_t$  and then conduct a vanilla training step to update the model parameter as  $\theta_t$ .

Our proposed strategy differs from previous CL works in two key aspects. **First**, our framework introduces a novel metric (FQS) to evaluate the forgery quality of deepfake samples. Additionally, we consider the model's dynamic feedback to achieve a more comprehensive assessment of forgery quality. In contrast, previous approaches [57], [59], [62] typically only consider using a certain indicator (which may not be specifically designed for deepfake data) to measure the difficulty level of samples and ignore either the static view or the dynamic view. **Second**, we introduce data augmentation to improve the quality of low-quality samples (those with a lower forgery quality score) after pacing the samples. Previous approaches do not further propose improving the lower score samples but use the higher score samples only.

## IV. EXPERIMENTS

### A. Experiment Settings

**Datasets.** In this paper, we train all models on the **FaceForensics++ (FF++)** [2] dataset. It contains 1,000 Pristine videos (i.e., the real sample) and 4,000 fake videos forged by four manipulation methods, i.e., Deepfakes (DF), Face2Face (F2F), FaceSwap (FS), NeuralTextures (NT). Besides, FF++ provides three quality levels in compression for these videos: raw, high-quality (HQ), and low-quality (LQ). The **HQ version of FF++** is adopted by default in this paper. If any deviation from this default, it will be explicitly stated. All samples within FF++ are split into training, validation, and testing sets at the video level following the official protocol.

For cross-dataset evaluation, we utilize four recent Deepfake datasets: **Celeb-DFv2 (CDF)** [19] employs advanced Deepfake algorithms on celebrity videos sourced from YouTube.

**Deepfake Detection Challenge Preview (DFDCp)** [14]: This dataset includes forgery videos featuring diverse ethnicities, ages, and genders. **Deepfake Detection Challenge Public Test Set (DFDC)** [20]: similar to DFDCp, this dataset contains videos with varied disturbance levels, such as compression, noise, and special effects, making it particularly challenging.

**WildDeepfake (Wild)** [13] contains 3,805 real face sequences and 3,509 fake face sequences collected from the internet. This collection includes a variety of synthesis methods, backgrounds, and character identities. For our experiments, we utilize the standard test set, which consists of 806 sequences.

**Implementation details.** As for pre-processing, we utilize MTCNN to detect and crop the face regions (enlarged by a factor of 1.3) from each video frame and resize them to

$256 \times 256$ . For each video, we select every ten frames to form the training dataset. We adopt Swin-Transformer-V2 Base (Swin-V2) [18] as the default backbone network, and the parameters are initialized by the weights pre-trained on the ImageNet1k. We employed the SGD optimizer with a cosine learning rate scheduler with  $\eta_{max} = 0.1$  (used in 5). We set 20 epoch for totally training, the pacing sequence  $\mathbf{T} = [2, 5, 8, 12, 15]$  and hyper-parameters  $\gamma = 0.9$  (used in 4),  $\alpha_\beta = 0.9$ ,  $E = 1000$ . The parameter  $\alpha_f$  is initialized at 0.5 and undergoes a reduction by half at each milestone.

**Evaluation Metrics.** In this work, we mainly report the area under the ROC curve (AUC) and accuracy (ACC) to compare with prior works. The video-level results are obtained by averaging predictions over each frame on an evaluated video.

### B. Performance Comparisons

1) *Intra-Dataset Comparisons*: In this section, we conduct comprehensive experiments on four different face processing methods listed in the FaceForensics++ dataset. We followed the same experimental setup as previous studies [35], [43], [63], training and testing our models on LQ DF, F2F, FS, and NT respectively. Table I shows the comparison results under video-level and image-level ACC. We have selected SPSL [40], which utilizes information from the frequency domain. Additionally, we chose models that have achieved state-of-the-art (SOTA) performance in our database within the past two years for comparison, including DL [43], DIL [63], FAMM [64], DDL [35] and Yin *et al.* [65]. The results show that our proposed method outperforms all compared methods in all cases except for FS, which is slightly worse than DDL. DDL uses a dynamic fine-grained difference capture module and a multi-scale spatio-temporal aggregation module to capture temporal inconsistency, which may overfit to the temporal inconsistency of the known manipulation methods. Consequently, the performance of DDL on CDF and DFDC is significantly inferior to our proposed method. In addition, our method outperforms DDL by 0.6% on average, which also proves the effectiveness of our method.

TABLE I  
FRAME-LEVEL (TOP) AND VIDEO-LEVEL (BOTTOM) AUC (%) ON  
FACEFORENSICS++ LQ DATASET WITH FOUR DIFFERENT MANIPULATION  
METHODS, i.e. DEEFAKES(DF), FACE2FACE (F2F), FACESWAP(FS),  
NEURALTEXTURES(NT). THE BOLD RESULTS ARE THE BEST. \*  
INDICATES OUR RE-IMPLEMENTATION OF THE EXISTING METHODS.

Methods	Venue	DF	F2F	FS	NT	Avg
DIL [63]	AAAI'22	86.78	70.85	81.59	57.64	74.22
DDL [35]	TIFS'23	97.43	92.28	<b>96.01</b>	79.35	91.27
FAMM [64]	TCSV'T23	90.00	91.00	92.75	85.50	89.81
Yin <i>et al.</i> [65]	TMM'24	94.75	92.19	88.49	73.87	87.33
Ours	-	<b>97.84</b>	<b>93.58</b>	95.56	<b>80.32</b>	<b>91.83</b>
SPSL* [40]	CVPR'21	96.79	91.79	96.43	82.88	91.97
Swin-V2* [18]	CVPR'22	97.50	89.64	93.57	83.93	91.16
DL [43]	TIFS'22	97.25	94.46	97.13	84.63	93.37
Ours	-	<b>99.29</b>	<b>96.42</b>	<b>97.15</b>	<b>86.07</b>	<b>94.73</b>

2) *Cross-manipulation Comparisons*: In real-world scenarios, predicting the methods used for face manipulation is often challenging. Therefore, it is crucial for our model to exhibit strong generalization capabilities to unseen manipulations.

TABLE II

IMAGE-LEVEL CROSS-MANIPULATION EVALUATION RESULTS (AUC).  
GREY BACKGROUND INDICATES INTRA-MANIPULATION RESULTS. THE  
BOLD RESULTS ARE THE BEST.

Methods	Train	Venue	DF	F2F	FS	NT	Avg.
RECCE [30]	DF	CVPR'22	<b>99.95</b>	69.75	54.72	77.15	75.39
CFM [47]		TIFS'24	99.93	<b>77.56</b>	54.94	75.04	76.87
Swin [18]		CVPR'22	99.66	65.86	52.77	76.53	73.71
Ours		-	99.41	75.32	<b>61.57</b>	<b>77.81</b>	<b>78.53</b>
RECCE [30]	F2F	CVPR'22	71.55	<b>99.20</b>	50.02	72.27	73.26
CFM [47]		TIFS'24	81.85	<b>99.23</b>	60.12	70.80	78.00
Swin [18]		CVPR'22	82.65	<b>99.23</b>	55.14	57.74	73.69
Ours		-	<b>93.94</b>	99.13	<b>64.86</b>	<b>78.43</b>	<b>84.09</b>
RECCE [30]	FS	CVPR'22	63.05	66.21	99.72	58.07	71.76
CFM [47]		TIFS'24	72.91	71.39	<b>99.85</b>	51.69	73.96
Swin [18]		CVPR'22	54.27	65.41	99.36	58.49	69.38
Ours		-	<b>84.31</b>	<b>82.97</b>	99.39	<b>67.74</b>	<b>83.60</b>
RECCE [30]	NT	CVPR'22	72.37	64.69	51.61	<b>99.59</b>	72.07
CFM [47]		TIFS'24	88.31	76.78	52.56	99.24	79.22
Swin [18]		CVPR'22	88.91	66.22	54.79	96.85	76.69
Ours		-	<b>94.62</b>	<b>83.99</b>	<b>56.73</b>	97.23	<b>83.14</b>

We conducted experiments using the FF++(HQ) dataset. We trained a model on one method from FF++ and tested it across all four methods (DF, F2F, FS, and NT). We select two state-of-the-art (SOTA) methods for comparison, including RECCE [30], CFM [47], and our baseline model Swin-V2 [18]. As shown in Table II, our proposed method can improve the average AUC by more than 10% compared with the baseline Swin-V2.

In addition, our method has comprehensive improvements over the SOTA method, which shows that our method has good generalization when detecting unseen manipulation methods.

3) *Cross-Datasets Comparisons*: The cross-datasets evaluation is still a challenging task because the unknown domain gap between the training and testing datasets can be caused by different source data, forgery methods, and/or post-processing. In this part, we evaluate generalization performance in a cross-dataset setting. Specifically, our models were trained on the FF++ and tested on CelebDF, Wild, DFDC-p, and DFDC, respectively. We compare our proposed method against twenty-three state-of-the-art DeepFake detectors in the past three years: RECCE [30], DL [43], SLADD [50], UIA-ViT [32], UCF [28], SFDG [41], NoiseDF [33], MSVT [44], FoCus [34], LSDA [9], DCL [46], CD-NeT [42], EFN4 + SBIs [10], DDL [35], SeeABLE [48], CDIN [45], TALL [36], AUNet [51], CADDMM [37], PIM [66], TDSCl [67], CFM [47] and DFDC [16]. The experimental results in terms of frame-level and video-level AUC are shown in Table III. It is evident that the proposed method lead to superior performance compared to other models in most cases, achieving the overall best results. All models are trained on the FF++ (C23) dataset for a fair comparison. We observe that our method surpasses the leading competitors in both frame-level and video-level evaluations. For instance, our approach surpasses TALL [36], which also employs Swin Transformer as its backbone network, by around 4% and 6% when testing on CDF and DFDC. The experimental results clearly highlight the significance of our method in enhancing the generalization capabilities of deepfake detectors.

TABLE III

FRAME-LEVEL (TOP) AND VIDEO-LEVEL (BOTTOM) AUC (%) OF CROSS-DATASETS PERFORMANCES COMPARED WITH SOTA METHODS.  
THE RESULTS OF PRIOR METHODS ARE DIRECTLY CITED FROM THE ORIGINAL PAPER AND THEIR SUBSEQUENCES FOR FAIR COMPARISON.  
THE BEST RESULTS ARE HIGHLIGHTED.

Methods	Venue	Type	Test Set AUC (%)			
			CDF	Wild	DFDCp	DFDC
RECCE [30]	CVPR'22	Frame	68.71	64.31	-	69.06
DL [43]	TIFS'22	Frame	70.65	-	-	63.31
SLADD [50]	CVPR'22	Frame	79.70	-	-	77.20
UIA-ViT [32]	ECCV'22	Frame	82.41	-	75.80	-
UCF [28]	ICCV'23	Frame	75.27	-	75.94	71.91
SFDG [41]	CVPR'23	Frame	75.83	<b>69.28</b>	-	73.64
NoiseDF [33]	AAAI'23	Frame	75.89	-	-	63.89
MSVT [44]	TCSVT'23	Frame	84.67	-	-	73.63
FoCus [34]	TIFS'24	Frame	76.13	73.31	76.62	68.42
LSDA [9]	CVPR'24	Frame	83.00	-	81.50	73.60
ProgressDet [68]	NeurIPS'24	Frame	84.48	-	81.16	72.40
Ours	-	Frame	<b>89.18</b>	<b>80.74</b>	<b>90.94</b>	<b>77.65</b>
DCL [46]	AAAI22	Video	82.30	71.14	-	76.71
CD-NeT [42]	ECCV'22	Video	88.50	-	-	77.00
EFNB4 + SBIs [10]	CVPR'22	Video	93.18	-	86.15	72.42
DDL [35]	TIFS'23	Video	71.36	-	-	73.08
SeeABLE [48]	CVPR'23	Video	87.30	-	86.30	75.90
CDIN [45]	TCSVT'23	Video	89.10	-	-	78.40
TALL [36]	ICCV'23	Video	90.79	-	-	76.78
AUNet [51]	CVPR'23	Video	92.77	-	86.16	73.82
CADDMM [37]	CVPR'23	Video	93.88	-	-	73.85
PIM [66]	TIFS'24	Video	87.34	72.28	80.69	68.04
TDSCl [67]	TCSVT'24	Video	89.06	78.93	-	80.85
CFM [47]	TIFS'24	Video	89.65	82.27	-	80.22
DFDC [16]	ICASSP'24	Video	82.26	71.75	90.63	72.37
Ours	-	Video	<b>94.75</b>	<b>83.77</b>	<b>93.41</b>	<b>82.04</b>

### C. Ablation Study

In this section, we conduct ablation studies on different components of the proposed model. All ablation studies are carried out on the HQ of FF++. Note that we aim to verify the effectiveness of the proposed methods targeted on the three research questions. We validate the effectiveness of both the static and dynamic forgery quality assessment strategies for **Question 1**, as given in Section IV-C4. We validate the effectiveness of the proposed FreDA for **Question 2**, as given in Section IV-C1. We validate the effectiveness of the proposed curriculum learning framework for **Question 3**, as given in Section IV-C3.

1) *Scalability and extensibility of FreDA*: FreDA augments data through splicing at the frequency domain level, and it can improve any data. Here, we combine FreDA with FF++, Blended images (BIs), and Self-Blended images (SBIs) to improve the data of BIs and SBIs and use these data for model training. The results are shown in Table IV. For the results of BIs and SBIs, we use the code provided by the author of the paper to reproduce. Since their paper uses RAW data for training, this paper uses The HQ version of FF++, so the performance is better than that of the original paper. The results show that the performance of combining BIs and FreDA is 4% higher in terms of AUC than that of BIs on average, the performance of combining SBIs and FreDA is 5% higher than that of SBIs on average, and the performance of combining FF++ and FreDA is 10% higher than that of FF++ on average. And the detection performance of all datasets has been improved. In addition, it is worth noting that BIs and SBIs have fewer forgery traces than FF++, while FreDA has

TABLE IV  
FREDA CAN IMPROVE THE GENERALIZATION OF MODELS TRAINED ON ALL TYPES OF DATA.

Methods	Celeb-DF	Wild	DFDC-p	DFDC	Avg
FF++	74.50	65.45	82.28	68.15	72.60
+FreDA	<b>83.95</b>	<b>76.20</b>	<b>93.95</b>	<b>77.41</b>	<b>82.88</b>
BiS	78.64	71.57	81.10	70.06	75.34
+FreDA	<b>82.28</b>	<b>72.87</b>	<b>91.87</b>	<b>73.99</b>	<b>80.25</b>
SBiS	88.63	63.85	80.01	66.85	74.84
+FreDA	<b>94.79</b>	<b>67.78</b>	<b>89.22</b>	<b>71.27</b>	<b>80.77</b>

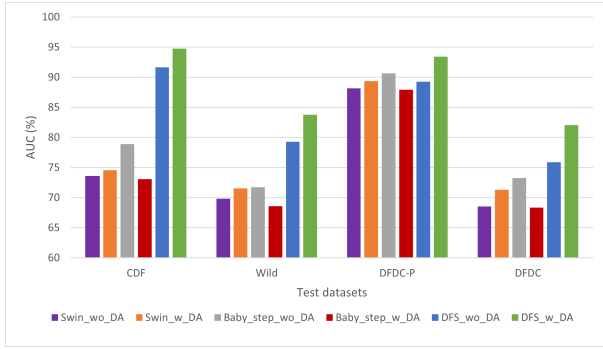


Fig. 6. Video-level AUC(%) on cross-datasets performance of different training strategies.

a greater improvement effect on FF++, which also verifies that FreDA has a greater effect on improving samples with obvious forgery traces. This also confirms the rationality of using FreDA on simple samples.

2) *Backbone impact*: In Table V, we evaluated the effect of different backbone architectures on the performance of our method, *i.e.*, Xception [12], EfficientNetB4 (EFNB4) [17]. We observe that our method can significantly improve the generalization performances of all evaluated models (at least 9% on average). Meanwhile, as our approach enhances data in a plug-and-play manner, the generalization performance can be improved across different backbones.

TABLE V  
VIDEO-LEVEL AUC(%) ON CROSS DATASET EVALUATIONS PERFORMANCES. THE BEST RESULTS ARE HIGHLIGHTED.

Methods	CDF	Wild	DFDC-p	DFDC	Avg
Xception	69.99	60.06	80.93	65.85	69.21
Ours	<b>82.75</b>	<b>72.29</b>	<b>89.00</b>	<b>70.83</b>	<b>78.72</b>
EFNB4	74.50	61.45	82.28	68.15	71.60
Ours	<b>86.05</b>	<b>77.09</b>	<b>89.95</b>	<b>75.57</b>	<b>82.17</b>

3) *Comparison with other training strategies*: In this part, we compared our method with other training strategies, including the vanilla training and BabyStep [57], [62] which is the simplest CL strategy that utilizes a static pre-defined hardness. We conducted BabyStep by introducing the IFQA score as the pre-defined hardness and utilizing the pacing setting in [69]. Furthermore, we also investigated the impacts of data augmentation. As shown in Figure 6, we observe that both the CL paradigm and data augmentation can improve

TABLE VI  
THE ABLATION STUDIES ON HARDNESS SCORES.

Methods	CDF	Wild	DFDCp	DFDC	Avg
baseline	74.53	71.56	89.37	71.30	76.69
Dynamic Loss	89.86	72.19	89.85	75.55	81.86
IFQA [16]	93.49	74.29	89.48	75.72	83.25
Ours	<b>94.75</b>	<b>83.77</b>	<b>93.41</b>	<b>82.04</b>	<b>88.49</b>

performance compared to vanilla training in most cases. However, introducing data augmentation in BabyStep suffers from performance degradation, as it makes the augmented data fail to match its pre-defined static hardness measure. This demonstrates that the dynamic CL strategy with data augmentation (*i.e.*, our method) is beneficial for generic deepfake detection. The key finding here is that the combination of a dynamic CL approach and data augmentation, as used in our method, is more effective than a static CL strategy with data augmentation. This suggests that the flexibility and responsiveness of the dynamic CL approach are crucial for leveraging data augmentation to improve deepfake detection performance.

4) *The impact of different definitions of hardness scores*: The definition of hardness score plays a crucial role in curriculum learning, so in this section, we use different kinds of hardness scores to conduct ablation experiments. We show the performance of vanilla training (baseline), using only Dynamic Loss, and using all scores (all) as the hardness definition, the results are shown in Table VI. It can be seen that by using DL as the definition of hardness scores, the generalization ability of the model can be greatly improved, achieving a 5.17% gain in terms of AUC than the model obtained by vanilla training. After the introduction of Arcface score, the AUC can be further improved by 3.75%.

After combining all the scores, the performance of the model is further improved, with an average detection performance of 88.49%. It shows that introducing the prior knowledge of and face recognition model (Arcface) helps to improve the definition of hardness score. Arcface score can improve hardness score from different perspectives, which also confirms our motivation to introduce these two static scores.

5) *The impact of the operation on easy samples*: Data augmentation is one of the important means of improving the generalization of the model. In this section, we evaluate the impact of different data augmentation on the model's generalization. We use three settings: no data augmentation (w/o DA), ordinary DA (such as JPEG compression, Gaussian Blur, Affine), and FreDA. The results are shown in Table VII. It can be seen that the generalization ability of the model can be improved by using simple data augmentation, with an average improvement of 2.85%, but there is an obvious decrease in CDF, with a performance reduction of 2.09%. When FreDA is performed on simple samples, the performance is improved across the board, with an average improvement of 7.85% compared to the setting without data augmentation. The results prove that data augmentation has a positive impact on the generalization ability of the model, and also proves the

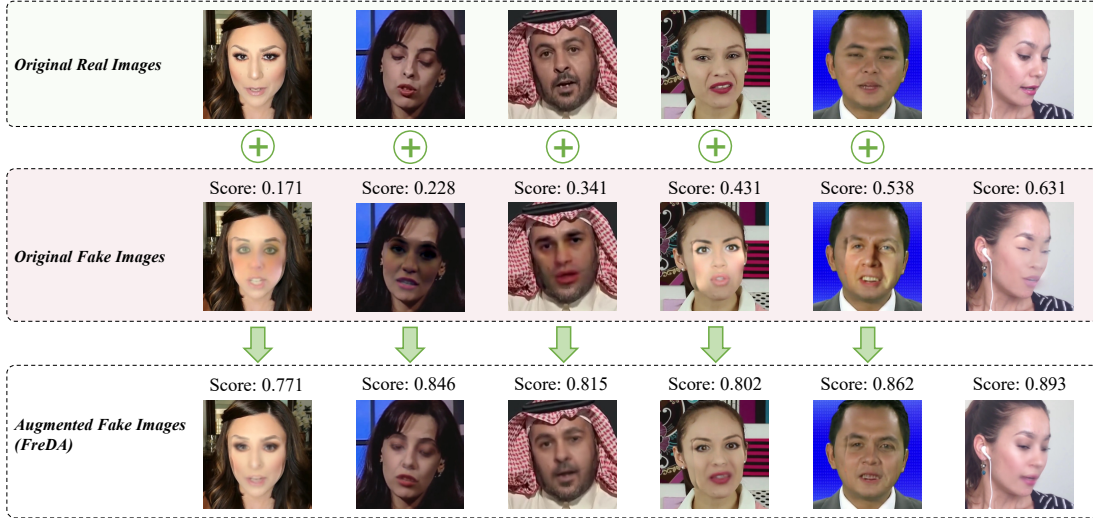


Fig. 7. Visualization of the fake data creation process of FreDA. FreDA enhances the realism (static scores) of the low-quality samples and generates corresponding high-quality samples.

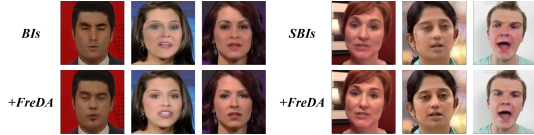


Fig. 8. Visualization of BIIs and SBIs data processed by FreDA. It can be observed that BIIs and SBIs data still have obvious forgery artifacts. After being processed by FreDA, the forged traces in the samples are significantly reduced.

TABLE VII  
THE ABLATION STUDIES ON OPERATION ON EASY SAMPLES.

Methods	CDF	Wild	DFDCp	DFDC	Avg
w/o DA	91.63	70.41	86.37	74.16	80.64
DA	89.54	79.26	89.26	75.89	83.49
FreDA	<b>94.75</b>	<b>83.77</b>	<b>93.41</b>	<b>82.04</b>	<b>88.49</b>

effectiveness of the FreDA we proposed.

#### D. Visualization

1) *Visualizations of FreDA samples*: We randomly screen out four low-quality samples with different ID similarity scores and process them with the FreDA module. The results are shown in Figure 7 and Figure 8. We can see that there are still samples with obvious artifacts of forgery in BIIs and SBIs. After being processed by FreDA, the visual quality of FF++, BIIs, and SBIs has been improved, and the static score of FF++ has also been greatly improved.

2) *Visualizations of hard samples and easy samples*: We explored the properties of samples with different hardness mined by method. Figure 9 illustrates samples with the highest and lowest FQS values. Fake faces with high FQS values are of relatively high visual quality and difficult to distinguish, while those with low FQS values display clearer forgery clues, such as color inconsistency and blending boundaries. For real faces, samples with high FQS values often undergo

TABLE VIII  
AVERAGE METRICS OF DIFFERENT FQS VALUES SAMPLES.

Method	idx	DF	F2F	FS	NT
		Top	3.22	3.26	2.32
TAR(%)	Bottom	8.59	9.03	12.32	5.87
	Top	3.22	3.26	2.32	5.71
SSIM	Bottom	0.9784	0.9932	0.9752	0.9821
	Top	0.9063	0.9361	0.9376	0.9673

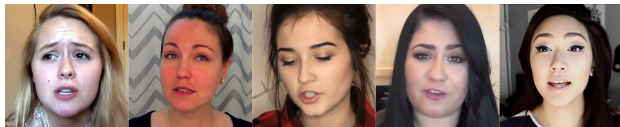
heavy post-processing, making them easily mistaken for fake faces. This demonstrates that the FQS values identified by our method align with human visual perception. We also computed the pixel-level tampering ratio (TAR, *i.e.*, the number of tampered pixels divided by the total number of pixels) and SSIM [70] metrics for fake samples with their corresponding real faces. As shown in Table VIII, fake faces with top FQS values involve low TAR and high SSIM, which indicates they have fewer forgery artifacts and higher similarities to the corresponding real faces. It makes sense that deepfake detectors would have difficulty in identifying these samples.

3) *ID similarity difference between FreDA images and original fake images*: We randomly selected 10 frames from each video, a total of 10,000 images, input these images and their corresponding real images into Arcface, and calculated the ID similarity score. After doing FreDA on these samples, we recalculate the ID similarity score. The comparison of ID similarity distribution is shown in Figure 10. We can see that after processing by the FreDA method, the overall quality of the image has improved, and the mean value has changed from the original 0.560 to the current 0.848, indicating that FreDA can improve the quality of the sample and turn low-quality samples into high-quality samples.

4) *Visualizations of sample hardness changes*: We explored the properties of our training process. We selected samples with the top (hard samples), bottom (easy samples), and median FQS values and illustrated the variations of their FQS values during the training. As shown in Figure 11, we



(a) Real faces with top FQS values



(b) Real faces with bottom FQS values



(c) Fake faces with top FQS values



(d) Fake faces with bottom FQS values

Fig. 9. Visualizations of top and bottom FQS values for real and fake faces on FF++(HQ).

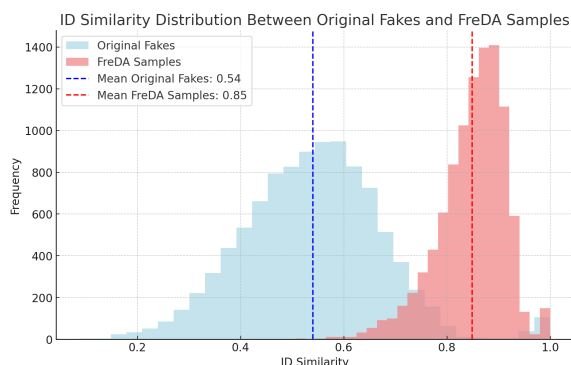


Fig. 10. The comparison of ID similarity distribution between original fake samples and FreDA samples.

can observe that the FQS values decrease throughout the training for all samples. We also found that the FQS values of easy samples remained small throughout the training. This is because deepfake detectors can learn to identify easy samples in the early stages of training, so our method does not tend to update their FQS. However, the detectors need more time to mine the forged clues of hard samples. This indicates that as learning continues, easy samples become less informative. Selecting and training on fewer hard samples is beneficial, as they provide more valuable information for the model to learn from and improve its performance. Our method allows the model to focus its attention on the hard samples that are more challenging and informative, leading to better overall performance compared to approaches that treat all samples equally or use a static curriculum strategy.

5) *Visualizations of learned latent space.*: We input real, original fake (ofake), and FreDA fake samples into a pre-

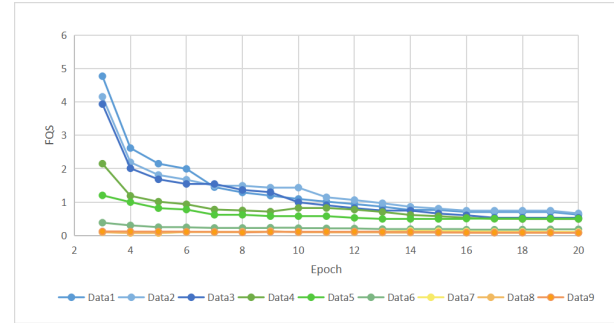


Fig. 11. Variations of FQS values during the training. We illustrate the change of 3 highest (Data 1-3), 3 lowest (Data 7-9), and random 3 median (Data 4-6) FQS values samples from the 3rd epoch.

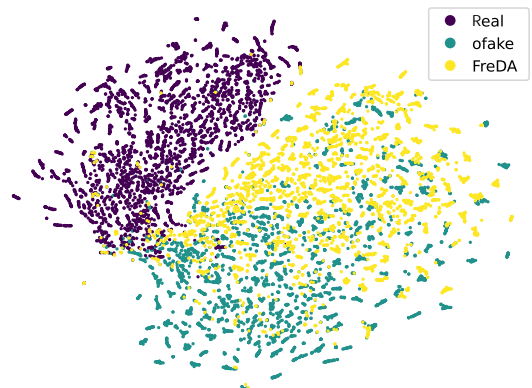


Fig. 12. t-SNE visualization of latent space with real, original fake (ofake), and FreDA (our augmentation version).

trained deepfake detector, and use t-SNE [71] to visualize the resulting features. The results are shown in Figure 12. It can be seen that the characteristics of fake images processed by the FreDA module are closer to real images than original fake images, indicating that the samples processed by FreDA are of higher quality and closer to real images.

6) *Discussion about Face Reenactment*: In this work, the scope for “Deepfake” is specifically the face swapping (FS). However, we also empirically verify that our method can also be applied to face reenactment (FR). Actually, FR is indeed more realistic than FS since FR can be also regarded as two same IDs for face-swapping in its generation process (thus achieving a higher score by our quality evaluator). Results in Tab. II show that our method can also work well for FR.

## V. CONCLUSION

This paper proposes a quality-centric framework that explicitly utilizes the forgery quality for generic deepfake detection. The Forgery Quality Score (FQS) is assessed statically via swapping pairs and dynamically based on the model’s feedback. Inspired by curriculum learning, we perform sample selection via FQS during training: a higher quality sample has a higher probability of being sampled for training the model. This manner aims to encourage the model to gradually learn more challenging samples, avoiding overfitting to easy-to-recognizable samples, thereby improving the generalization

performance. Furthermore, for these low-quality fake data, we propose a frequency data augmentation method called FreDA, which aims to reduce the easy artifacts of these samples and enhance their realism at the frequency level. Extensive experiments prove that our method can be applied to other approaches in a plug-and-play manner, and can largely improve the generalization of the baseline model. The main limitation of our approach lies in the assumption that obtaining real-fake paired data with the same background is feasible. The assumption is reasonable as in practice, it is possible to conduct such data collection. For example, in the construction of many existing datasets, real and fake images with the same background are often included. This shows that obtaining real-fake paired data with the same background can be achieved in real scenarios. In the future, we aim to explore scenarios where obtaining paired data is not feasible and focus on developing more general forgery quality assessment methods as well as other data augmentation techniques.

## REFERENCES

- [1] D. Afchar, V. Nozick, J. Yamagishi, and I. Echizen, “MesoNet: A Compact Facial Video Forgery Detection Network,” in *2018 IEEE International Workshop on Information Forensics and Security*, 2018, pp. 1–7.
- [2] A. Rossler, D. Cozzolino, L. Verdoliva, C. Riess, J. Thies, and M. Niesser, “FaceForensics++: Learning to Detect Manipulated Facial Images,” in *Proceedings of the IEEE/CVF International Conference on Computer Vision*, 2019, pp. 1–11.
- [3] S. Cao, Q. Zou, X. Mao, D. Ye, and Z. Wang, “Metric Learning for Anti-Compression Facial Forgery Detection,” in *Proceedings of the 29th ACM International Conference on Multimedia*, 2021, pp. 1929–1937.
- [4] Z. Gu, Y. Chen, T. Yao, S. Ding, J. Li, F. Huang, and L. Ma, “Spatiotemporal Inconsistency Learning for Deepfake Video Detection,” in *Proceedings of the 29th ACM International Conference on Multimedia*, 2021, pp. 3473–3481.
- [5] S. A. Khan and H. Dai, “Video Transformer for Deepfake Detection with Incremental Learning,” in *Proceedings of the 29th ACM International Conference on Multimedia*, 2021, pp. 1821–1828.
- [6] M. Kim, S. Tariq, and S. S. Woo, “CORED: Generalizing Fake Media Detection with Continual Representation Using Distillation,” in *Proceedings of the 29th ACM International Conference on Multimedia*, 2021, pp. 337–346.
- [7] L. Li, J. Bao, T. Zhang, H. Yang, D. Chen, F. Wen, and B. Guo, “Face X-Ray for More General Face Forgery Detection,” in *Proceedings of the IEEE/CVF Conference on Computer Vision and Pattern Recognition*, 2020, pp. 5001–5010.
- [8] R. Geirhos, J.-H. Jacobsen, C. Michaelis, R. Zemel, W. Brendel, M. Bethge, and F. A. Wichmann, “Shortcut Learning in Deep Neural Networks,” *Nature Machine Intelligence*, vol. 2, no. 11, pp. 665–673, 2020.
- [9] Z. Yan, Y. Luo, S. Lyu, Q. Liu, and B. Wu, “Transcending Forgery Specificity with Latent Space Augmentation for Generalizable Deepfake Detection,” in *Proceedings of the IEEE/CVF Conference on Computer Vision and Pattern Recognition*, 2024, pp. 8984–8994.
- [10] K. Shiohara and T. Yamasaki, “Detecting Deepfakes with Self-Blended Images,” in *Proceedings of the IEEE/CVF Conference on Computer Vision and Pattern Recognition*, 2022, pp. 18720–18729.
- [11] L. Trinh and Y. Liu, “An Examination of Fairness of AI Models for Deepfake Detection,” *arXiv preprint arXiv:2105.00558*, 2021.
- [12] F. Chollet, “Xception: Deep Learning With Depthwise Separable Convolutions,” in *Proceedings of the IEEE Conference on Computer Vision and Pattern Recognition*, 2017, pp. 1251–1258.
- [13] B. Zi, M. Chang, J. Chen, X. Ma, and Y.-G. Jiang, “WildDeepfake: A Challenging Real-World Dataset for Deepfake Detection,” in *Proceedings of the 28th ACM International Conference on Multimedia*, 2020, pp. 2382–2390.
- [14] B. Dolhansky, R. Howes, B. Pflaum, N. Baram, and C. C. Ferrer, “The Deepfake Detection Challenge (DFDC) Preview Dataset,” *arXiv preprint arXiv:1910.08854*, 2019.
- [15] J. Deng, J. Guo, N. Xue, and S. Zafeiriou, “ArcFace: Additive Angular Margin Loss for Deep Face Recognition,” in *Proceedings of the IEEE/CVF Conference on Computer Vision and Pattern Recognition*, 2019, pp. 4690–4699.
- [16] W. Song, Y. Lin, and B. Li, “Towards Generic Deepfake Detection with Dynamic Curriculum,” in *ICASSP 2024-2024 IEEE International Conference on Acoustics, Speech and Signal Processing*. IEEE, 2024, pp. 4500–4504.
- [17] M. Tan and Q. Le, “EfficientNet: Rethinking Model Scaling for Convolutional Neural Networks,” in *International Conference on Machine Learning*. PMLR, 2019, pp. 6105–6114.
- [18] Z. Liu, H. Hu, Y. Lin, Z. Yao, Z. Xie, Y. Wei, J. Ning, Y. Cao, Z. Zhang, L. Dong, F. Wei, and B. Guo, “Swin Transformer V2: Scaling Up Capacity and Resolution,” in *Proceedings of the IEEE/CVF Conference on Computer Vision and Pattern Recognition*, 2022, pp. 12009–12019.
- [19] Y. Li, X. Yang, P. Sun, H. Qi, and S. Lyu, “Celeb-DF: A Large-Scale Challenging Dataset for DeepFake Forensics,” in *Proceedings of the IEEE/CVF Conference on Computer Vision and Pattern Recognition*, 2020, pp. 3207–3216.
- [20] B. Dolhansky, J. Bitton, B. Pflaum, J. Lu, R. Howes, M. Wang, and C. C. Ferrer, “The Deepfake Detection Challenge (DFDC) Dataset,” *arXiv preprint arXiv:2006.07397*, 2020.
- [21] Y. Li, M. Chang, and S. Lyu, “In Ictu Oculi: Exposing AI Created Fake Videos by Detecting Eye Blinking,” in *2018 IEEE International Workshop on Information Forensics and Security*, 2018, pp. 1–7.
- [22] X. Yang, Y. Li, and S. Lyu, “Exposing Deep Fakes Using Inconsistent Head Poses,” in *ICASSP 2019 - 2019 IEEE International Conference on Acoustics, Speech and Signal Processing*, 2019, pp. 8261–8265.
- [23] Y. Li and S. Lyu, “Exposing DeepFake Videos By Detecting Face Warping Artifacts,” in *Proceedings of the IEEE/CVF Conference on Computer Vision and Pattern Recognition Workshops*, 2019, pp. 46–52.
- [24] H. Zhao, W. Zhou, D. Chen, T. Wei, W. Zhang, and N. Yu, “Multi-Attentional Deepfake Detection,” in *Proceedings of the IEEE/CVF Conference on Computer Vision and Pattern Recognition*, 2021, pp. 2185–2194.
- [25] Y. Luo, Y. Zhang, J. Yan, and W. Liu, “Generalizing Face Forgery Detection with High-Frequency Features,” in *Proceedings of the IEEE/CVF Conference on Computer Vision and Pattern Recognition*, 2021, pp. 16317–16326.
- [26] Z. Yan, Y. Zhang, X. Yuan, S. Lyu, and B. Wu, “Deepfakebench: A Comprehensive Benchmark of Deepfake Detection,” *arXiv preprint arXiv:2307.01426*, 2023.
- [27] Z. Yan, T. Yao, S. Chen, Y. Zhao, X. Fu, J. Zhu, D. Luo, L. Yuan, C. Wang, S. Ding et al., “DF40: Toward Next-Generation Deepfake Detection,” *arXiv preprint arXiv:2406.13495*, 2024.
- [28] Z. Yan, Y. Zhang, Y. Fan, and B. Wu, “UCF: Uncovering Common Features for Generalizable Deepfake Detection,” in *Proceedings of the IEEE/CVF International Conference on Computer Vision*, 2023, pp. 22412–22423.
- [29] J. Liang, H. Shi, and W. Deng, “Exploring Disentangled Content Information for Face Forgery Detection,” in *Computer Vision – ECCV 2022*, 2022, pp. 128–145.
- [30] J. Cao, C. Ma, T. Yao, S. Chen, S. Ding, and X. Yang, “End-to-End Reconstruction-Classification Learning for Face Forgery Detection,” in *Proceedings of the IEEE/CVF Conference on Computer Vision and Pattern Recognition*, 2022, pp. 4113–4122.
- [31] C. Wang and W. Deng, “Representative Forgery Mining for Fake Face Detection,” in *Proceedings of the IEEE/CVF Conference on Computer Vision and Pattern Recognition*, 2021, pp. 14923–14932.
- [32] W. Zhuang, Q. Chu, Z. Tan, Q. Liu, H. Yuan, C. Miao, Z. Luo, and N. Yu, “UIA-ViT: Unsupervised Inconsistency-Aware Method Based on Vision Transformer for Face Forgery Detection,” in *Computer Vision – ECCV 2022*, 2022, pp. 391–407.
- [33] T. Wang and K. P. Chow, “Noise Based Deepfake Detection via Multi-Head Relative-Interaction,” *Proceedings of the AAAI Conference on Artificial Intelligence*, vol. 37, no. 12, pp. 14 548–14 556, 2023.
- [34] J. Tian, P. Chen, C. Yu, X. Fu, X. Wang, J. Dai, and J. Han, “Learning to Discover Forgery Cues for Face Forgery Detection,” *IEEE Transactions on Information Forensics and Security*, 2024.
- [35] Q. Yin, W. Lu, B. Li, and J. Huang, “Dynamic Difference Learning with Spatio-Temporal Correlation for Deepfake Video Detection,” *IEEE Transactions on Information Forensics and Security*, 2023.
- [36] Y. Xu, J. Liang, G. Jia, Z. Yang, Y. Zhang, and R. He, “TALL: Thumbnail Layout for Deepfake Video Detection,” in *Proceedings of the IEEE/CVF International Conference on Computer Vision*, 2023, pp. 22658–22668.

[37] S. Dong, J. Wang, R. Ji, J. Liang, H. Fan, and Z. Ge, "Implicit Identity Leakage: The Stumbling Block to Improving Deepfake Detection Generalization," in *Proceedings of the IEEE/CVF Conference on Computer Vision and Pattern Recognition*, 2023, pp. 3994–4004.

[38] Y. Qian, G. Yin, L. Sheng, Z. Chen, and J. Shao, "Thinking in Frequency: Face Forgery Detection by Mining Frequency-Aware Clues," in *Computer Vision - ECCV 2020*, 2020, pp. 86–103.

[39] R. Durall, M. Keuper, and J. Keuper, "Watch Your Up-Convolution: CNN Based Generative Deep Neural Networks are Failing to Reproduce Spectral Distributions," in *Proceedings of the IEEE/CVF Conference on Computer Vision and Pattern Recognition*, 2020, pp. 7890–7899.

[40] H. Liu, X. Li, W. Zhou, Y. Chen, Y. He, H. Xue, W. Zhang, and N. Yu, "Spatial-Phase Shallow Learning: Rethinking Face Forgery Detection in Frequency Domain," in *Proceedings of the IEEE/CVF Conference on Computer Vision and Pattern Recognition*, 2021, pp. 772–781.

[41] Y. Wang, K. Yu, C. Chen, X. Hu, and S. Peng, "Dynamic Graph Learning with Content-Guided Spatial-Frequency Relation Reasoning for Deepfake Detection," in *Proceedings of the IEEE/CVF Conference on Computer Vision and Pattern Recognition*, 2023, pp. 7278–7287.

[42] L. Song, Z. Fang, X. Li, X. Dong, Z. Jin, Y. Chen, and S. Lyu, "Adaptive Face Forgery Detection in Cross Domain," in *Computer Vision - ECCV 2022*, 2022, pp. 467–484.

[43] C. Kong, B. Chen, H. Li, S. Wang, A. Rocha, and S. Kwong, "Detect and Locate: Exposing Face Manipulation by Semantic-and Noise-Level Telltales," *IEEE Transactions on Information Forensics and Security*, vol. 17, pp. 1741–1756, 2022.

[44] Y. Yu, R. Ni, Y. Zhao, S. Yang, F. Xia, N. Jiang, and G. Zhao, "MSVT: Multiple Spatiotemporal Views Transformer for DeepFake Video Detection," *IEEE Transactions on Circuits and Systems for Video Technology*, vol. 33, no. 9, pp. 4462–4471, 2023.

[45] H. Wang, Z. Liu, and S. Wang, "Exploiting Complementary Dynamic Incoherence for DeepFake Video Detection," *IEEE Transactions on Circuits and Systems for Video Technology*, vol. 33, no. 8, pp. 4027–4040, 2023.

[46] K. Sun, T. Yao, S. Chen, S. Ding, J. Li, and R. Ji, "Dual Contrastive Learning for General Face Forgery Detection," in *Proceedings of the AAAI Conference on Artificial Intelligence*, vol. 36, 2022, pp. 2316–2324.

[47] A. Luo, C. Kong, J. Huang, Y. Hu, X. Kang, and A. C. Kot, "Beyond the Prior Forgery Knowledge: Mining Critical Clues for General Face Forgery Detection," *IEEE Transactions on Information Forensics and Security*, vol. 19, pp. 1168–1182, 2023.

[48] N. Larue, N.-S. Vu, V. Struc, P. Peer, and V. Christopides, "SeeABLE: Soft Discrepancies and Bounded Contrastive Learning for Exposing Deepfakes," in *Proceedings of the IEEE/CVF International Conference on Computer Vision*, 2023, pp. 21011–21021.

[49] T. Zhao, X. Xu, M. Xu, H. Ding, Y. Xiong, and W. Xia, "Learning Self-Consistency for Deepfake Detection," in *Proceedings of the IEEE/CVF International Conference on Computer Vision*, 2021, pp. 15023–15033.

[50] L. Chen, Y. Zhang, Y. Song, L. Liu, and J. Wang, "Self-Supervised Learning of Adversarial Example: Towards Good Generalizations for Deepfake Detection," in *Proceedings of the IEEE/CVF Conference on Computer Vision and Pattern Recognition*, 2022, pp. 18710–18719.

[51] W. Bai, Y. Liu, Z. Zhang, B. Li, and W. Hu, "AUNet: Learning Relations Between Action Units for Face Forgery Detection," in *Proceedings of the IEEE/CVF Conference on Computer Vision and Pattern Recognition*, 2023, pp. 24709–24719.

[52] Z. Wang, J. Bao, W. Zhou, W. Wang, and H. Li, "AltFreezing for More General Video Face Forgery Detection," in *Proceedings of the IEEE/CVF Conference on Computer Vision and Pattern Recognition*, 2023, pp. 4129–4138.

[53] Z. Yan, Y. Zhao, S. Chen, X. Fu, T. Yao, S. Ding, and L. Yuan, "Generalizing Deepfake Video Detection with Plug-and-Play: Video-Level Blending and Spatiotemporal Adapter Tuning," *arXiv preprint arXiv:2408.17065*, 2024.

[54] B. M. Le and S. S. Woo, "Quality-Agnostic Deepfake Detection with Intra-Model Collaborative Learning," in *Proceedings of the IEEE/CVF International Conference on Computer Vision*, 2023, pp. 22378–22389.

[55] H. Kim, J. Lee, L. H. Park, and T. Kwon, "On the Correlation between Deepfake Detection Performance and Image Quality Metrics," in *Proceedings of the 3rd ACM Workshop on the Security Implications of Deepfakes and Cheapfakes*, 2024, pp. 14–19.

[56] S. Lee, J. An, and S. S. Woo, "BZNet: Unsupervised Multi-Scale Branch Zooming Network for Detecting Low-Quality Deepfake Videos," in *Proceedings of the ACM Web Conference 2022*, 2022, pp. 3500–3510.

[57] V. Cirik, E. Hovy, and L.-P. Morency, "Visualizing and Understanding Curriculum Learning for Long Short-Term Memory Networks," *arXiv preprint arXiv:1611.06204*, 2016.

[58] V. I. Spitkovsky, H. Alshawi, and D. Jurafsky, "Baby Steps: How 'Less is More' in Unsupervised Dependency Parsing," *NIPS: Grammar Induction, Representation of Language and Language Learning*, pp. 1–10, 2009.

[59] Y. Wang, W. Gan, J. Yang, W. Wu, and J. Yan, "Dynamic Curriculum Learning for Imbalanced Data Classification," in *Proceedings of the IEEE/CVF International Conference on Computer Vision*, 2019, pp. 5017–5026.

[60] M. Kumar, B. Packer, and D. Koller, "Self-Paced Learning for Latent Variable Models," *Advances in Neural Information Processing Systems*, vol. 23, 2010.

[61] Y. Kong, L. Liu, J. Wang, and D. Tao, "Adaptive Curriculum Learning," in *Proceedings of the IEEE/CVF International Conference on Computer Vision*, 2021, pp. 5067–5076.

[62] Y. Bengio, J. Louradour, R. Collobert, and J. Weston, "Curriculum Learning," in *Proceedings of the 26th Annual International Conference on Machine Learning*, 2009, pp. 41–48.

[63] Z. Gu, Y. Chen, T. Yao, S. Ding, J. Li, and L. Ma, "Delving into the Local: Dynamic Inconsistency Learning for Deepfake Video Detection," in *Proceedings of the AAAI Conference on Artificial Intelligence*, vol. 36, no. 1, 2022, pp. 744–752.

[64] X. Liao, Y. Wang, T. Wang, J. Hu, and X. Wu, "FAMM: Facial Muscle Motions for Detecting Compressed Deepfake Videos over Social Networks," *IEEE Transactions on Circuits and Systems for Video Technology*, vol. 33, no. 12, pp. 7236–7251, 2023.

[65] Z. Yin, J. Wang, Y. Xiao, H. Zhao, T. Li, W. Zhou, A. Liu, and X. Liu, "Improving Deepfake Detection Generalization by Invariant Risk Minimization," *IEEE Transactions on Multimedia*, vol. 26, pp. 6785–6798, 2024.

[66] W. Guan, W. Wang, J. Dong, and B. Peng, "Improving Generalization of Deepfake Detectors by Imposing Gradient Regularization," *IEEE Transactions on Information Forensics and Security*, 2024.

[67] R. Zhang, P. He, H. Li, S. Wang, and Y. Cao, "Temporal Diversified Self-Contrastive Learning for Generalized Face Forgery Detection," *IEEE Transactions on Circuits and Systems for Video Technology*, pp. 1–1, 2024.

[68] J. Cheng, Z. Yan, Y. Zhang, Y. Luo, Z. Wang, and C. Li, "Can We Leave Deepfake Data Behind in Training Deepfake Detector?" *arXiv preprint arXiv:2408.17052*, 2024.

[69] G. Hacohen and D. Weinshall, "On The Power of Curriculum Learning in Training Deep Networks," in *Proceedings of the 36th International Conference on Machine Learning*, 2019, pp. 2535–2544.

[70] Z. Wang, A. C. Bovik, H. R. Sheikh, and E. P. Simoncelli, "Image Quality Assessment: From Error Visibility to Structural Similarity," *IEEE transactions on Image Processing*, vol. 13, no. 4, pp. 600–612, 2004.

[71] L. Van der Maaten and G. Hinton, "Visualizing Data Using T-SNE," *Journal of Machine Learning Research*, vol. 9, no. 11, 2008.